Zachary Gagnon
Jason Gordon
Shramik Sengupta
Hsueh-Chia Chang

Department of Chemical and Biomolecular Engineering, Center for Microfluidics and Medical Diagnostics, University of Notre Dame, Notre Dame, IN, USA

Received August 13, 2007
Revised December 5, 2007
Accepted January 7, 2008

Research Article

Bovine red blood cell starvation age discrimination through a glutaraldehyde-amplified dielectrophoretic approach with buffer selection and membrane cross-linking

We report a novel buffer electric and dielectric relaxation time tuning technique, coupled with a glutaraldehyde (Glt.) cross-linking cell fixation reaction that allows for sensitive dielectrophoretic analysis and discrimination of bovine red blood cells of different starvation age. Guided by a single-shell oblate spheroid model, a zwitterion buffer composition is selected to ensure that two measurable crossover frequencies (cof's) near 500 kHz exist for dielectrophoresis (DEP) within a small range of each other. It is shown that the low cof is sensitive to changes in the cell membrane dielectric constant, in which cross-linking by Glt. reduces the dielectric constant of the cell membrane from 10.5 to 3.8, while the high cof is sensitive to cell cytoplasm conductivity changes. We speculate that this enhanced particle polarizability that results from the cross-linking reaction is because younger (reduced starvation time) cells possess more amino groups that the reaction can release to enhance the cell interior ionic strength. Such sensitive discrimination of cells with different age (surface protein density) by DEP is not possible without the zwitterion buffer and cleavage by Glt. treatment. It is then expected that rapid identification and sorting of healthy from diseased cells can be similarly sensitized.

Keywords:
Crossover frequency / Dielectrophoresis / Glutaraldehyde / Red blood cell
DOI 10.1002/elps.200700604

1 Introduction

Dielectrophoresis (DEP) is a term commonly used to describe the field-induced polarization and translational motion of a polarizable particle in a nonuniform alternating current (AC) electric field [1]. In recent years, much work has been done attempting to utilize and integrate DEP into microfluidic devices for particle and cellular manipulation. Different types of cells and/or bacteria are expected to have distinctly diverse osmotic pressures, internal ionic strengths, size, geometry, action potentials, and membrane protein densities. As such, their polarization under an AC electric field should also be quite unique because of these distinct electric and dielectric signatures. DEP could hence allow for selective sorting and potentially identification. Because the DEP microelectrodes can be easily implemented into small microchannel geometries, DEP has been successfully used to concentrate, selectively trap, separate, and sort microsized and nanosized particles, immunocolloids, bacteria, and a large variety of eukaryotic cells in microchip applications [2–5].

Much work has been done in chemical modification of both cells and the suspending buffer in order to optimize the desired cellular dielectrophoretic response [4, 6–11]. We have recently introduced the concept of membrane cross-linking-induced dielectrophoretic discrimination of bovine red blood cells (bRBCs) [12]. The intention behind this work is to amplify differences in bRBC signatures through membrane cross-linking and to further study and model the physical effects that glutaraldehyde (Glt.) has on the electrical properties of the bRBCs and how this impacts their corresponding dielectrophoretic behavior.

Correpondence: Professor Hsueh-Chia Chang, 182 Fitzpatrick Hall, Department of Chemical Engineering, University of Notre Dame, Notre Dame, IN 46556, USA
E-mail: hchang@nd.edu
Fax: +1-574-631-8366

Abbreviations: AC, alternating current; **bRBC,** bovine red blood cell; **cof,** crossover frequency; **DEP,** dielectrophoresis; **Glt.,** glutaraldehyde

2 Theory

2.1 Dielectrophoresis

The classical theory models the DEP force F_{DEP} induced by an AC field, E, with frequency ω, on a spherical particle of radius a as [1]

$$F_{\mathrm{DEP}} = 2\pi a^3 \varepsilon_{\mathrm{m}} Re(f_{\mathrm{CM}}) \nabla |E|^2 \quad (1)$$

where ε_{m} is the real part of the permittivity of the suspending medium, and $\varepsilon_{\mathrm{p}}^*$ and $\varepsilon_{\mathrm{m}}^*$ are the complex permittivities of the particle and the medium, respectively, and are each described by $\varepsilon^* = \varepsilon + \sigma/(i\omega)$. For a shell-less lossy dielectric sphere, the factor $f_{\mathrm{CM}} = (\varepsilon_{\mathrm{p}}^* - \varepsilon_{\mathrm{m}}^*)/(\varepsilon_{\mathrm{p}}^* + 2\varepsilon_{\mathrm{m}}^*)$ is the frequency-dependent Clausius–Mossotti (CM) factor. This equation reveals that the permittivity dominates particle polarization at high frequency, while the conductivity σ becomes the governing factor at low frequency. A positive CM factor indicates that the DEP force pushes a polarized particle toward a local electric field maximum, which is known as positive DEP (pDEP), while a negative CM factor pushes the particle away from the field maximum and into regions of weak electric field, which is known as negative DEP (nDEP). The frequency at which the CM factor equals zero, which is at the point where the induced molecular particle dipole cancels out the conductive dispersive dipole, is known as the cross-over frequency (cof) [1]. As conductive polarization involves migrating ions, it is a relatively slow phenomenon. On the other hand, dielectric polarization involves relatively fast charge segregation at the molecular level. Consequently, conductive polarization is favored at low frequencies while dielectric polarization dominates at high frequencies. The cof hence demarcates these two distinct polarization mechanisms. For particles with particle conductivity higher and permittivity lower than that of the medium, pDEP is expected below the cof and nDEP above it according to this simple model. Most cells and bacteria do have lower permittivity than any electrolyte buffer, and lowering the buffer conductivity to values smaller than that of the cell interior should hence produce this expected single cof behavior. However, due to the nature of the cell membrane, the classical model must be modified in order to describe RBC polarization mechanics, which exhibit two cof's.

2.2 DEP-shell model

As proposed by Hoeber [13], a red blood cell (RBC) cannot simply be described by the lossy dielectric sphere model, but is, however, well described as an oblate sphere of highly conducting cytoplasm surrounded by an insulating membrane. Irimajiri *et al.* [14] later combined this model with a multi-shelled Maxwell–Wagner (MW) theory in order to approximate the dielectric polarization of biological cells suspended in an electrolyte solution. As shown in Fig. 1, an RBC is approximated as a single-shell oblate sphere, where the cytoplasm is bound by a membrane of finite thickness, $d_{\mathrm{mem}} \sim 8$ nm, radius *r*, height c, and half-length *a*. Each interface that separates the different dielectric layers introduces an MW relaxation process, and thus allows for the possibility of multiple cof's for even a single-shell cell with two interfaces, an inner cytoplasm/membrane, and an outer media/membrane. If the shell is very conductive, which would be the case for cells with high ion-channel activity, the membrane can be lumped with the cytoplasm (similar to the conducting Stern layer theory of latex particles [2]), and the shell model reduces to the previous shell-less model. Hence, the membrane can only fundamentally change the cell's DEP behavior if its conductivity is low, which then means that it behaves like a pure dielectric membrane with a large capacitance. In the work described here, we tune the membrane permittivity and the buffer and cytoplasm conductivities in order to elicit these two distinct relaxation dynamics.

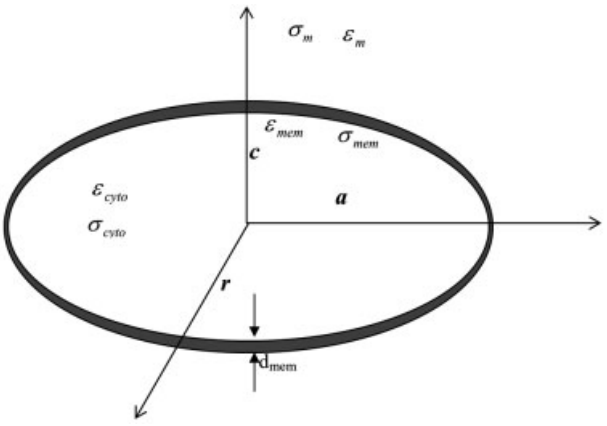

Figure 1. Single-shell oblate spheroid model of a red blood cell.

When multiple cof's exist, each individual one is sensitive to charge relaxation at a specific interface. We seek a particular cof for the internal interface of the membrane, as we expect the relaxation time there is most sensitive to the starvation age and health of the RBC. The induced dipole direction of a RBC will depend on the electrical properties of both the membrane and cell interior. These parameters have been well reported in the literature and have typically been determined *via* RBC electrorotation experiments [15]. A typical RBC suspended in an aqueous medium of 0.85% NaCl ($\varepsilon_{\mathrm{m}} \sim 80$, $\sigma_{\mathrm{m}} \sim 12$ mS/cm) has a reported membrane conductivity σ_{mem} and relative permittivity $\varepsilon_{\mathrm{mem}}$ of $<10^{-7}$ S/m and 10.5, respectively, and an interior conductivity and permittivity of 310 mS/m and ~60, respectively. The thin (thickness of $d = 8$ nm) dielectric membrane fundamentally changes the particle-induced dipole, DEP mobility, and cof. As the membrane capacitance is $\varepsilon_{\mathrm{mem}}/d$, its capacitance is much higher than that of the particle. The charge relaxation time is then the RC (resistor–capacitor) relaxation time when this membrane capacitor is coupled to a conductive medium (resistor) on one side. At a sufficiently low frequency that permits conductive polarization to dominate over dielectric polarization, the conductive charging of the RBC membrane with a large capacitance will produce a large polarization across the membrane. As the interior cytoplasm conductivity is higher than the medium conductivity, the membrane polarization that results produces a field that opposes and screens the external field, thus preventing field penetration into the cell interior. Therefore, the resulting DEP dipole will be governed by differences in medium (larger) and mem-

brane (smaller) conductivity, resulting in nDEP. If the AC frequency is increased such that it exceeds the inverse RC time of the polarized membrane/media interface, typically on the order of $\sim\sigma_m/\varepsilon_{mem}$, field penetration into the cytoplasm interior will occur, resulting in a DEP dipole that now depends on the conductivity of the cytoplasm (larger) and the medium (smaller). Thus, the DEP dipole will change direction and point toward regions of high field intensity (pDEP). Finally, if one increases the frequency to a point that exceeds the inverse RC time of the media/cytoplasm, $\sim\sigma_{cyto}/\varepsilon_m$, dielectric charge relaxation and ion migration *via* conductive polarization will not have enough time to take place, and thus the resulting dipole will be regulated by permittivity differences between the cell interior and the bulk medium. With a medium permittivity that is higher than that of the cytoplasm, the exterior of the cell will polarize to a greater extent to again reverse the dipole direction, producing an nDEP behavior. Hence, the large capacitance of the thin dielectric membrane with its unique screening effect produces two cof's that are sensitively dependent on the membrane permittivity. This is in direct contrast to cells with a conducting membrane that have only one cof. Based on this analysis, a single-shell RBC has the ability to exhibit two distinct cof's, one at low frequency, cof_1, that is governed by the relaxation time of the media/membrane, and one at high frequency, cof_2, that is dependent on the relaxation time of the media/cytoplasm. Therefore, it becomes possible to probe both the membrane and the cell interior by measuring both cof_1 and the cof_2 of a RBC. We expect the higher cof, cof_2, with its sensitivity to cytoplasm conductivity to be sensitive to the age and health or the RBC.

As the CM factor used in the DEP force expression (Eq. 1) is valid only for homogeneous spherical particles, it is necessary to modify this factor taking into account both the spheroidal shape and the low-conductive cell membrane of the bRBC. Here, we better approximate the biconcave shape of a RBC as an oblate spheroid. For the case of a single-shell oblate spheroid with major axis aligned parallel with the applied field, the CM factor can be shown to be [15]

$$K(\omega) = V_c\varepsilon_m \frac{\varepsilon_p^{'} - \varepsilon_m^*}{(\varepsilon_p^{'} - \varepsilon_m^*)A_{op} + \varepsilon_m^*} \tag{2}$$

The parameter A_{op} describes the geometry specific degree to which the exterior of the cell, from the outer membrane edge to infinity, depolarizes along the principal axis, V_c represents the cell volume, and $\varepsilon_p^{'}$ is the effective permittivity of the particle given by

$$\varepsilon_p^{'} = \varepsilon_{mem}^* \frac{\varepsilon_{mem}^* + (\varepsilon_{cyto}^* - \varepsilon_{mem}^*)[A_{ip} + \nu(1 - A_{op})]}{\varepsilon_{mem}^* + (\varepsilon_{cyto}^* - \varepsilon_{mem}^*)[A_{ip} - \nu A_{op}]} \tag{3}$$

where ε_{mem}^* and ε_{int}^* are the complex permittivity's of the cell membrane and interior, respectively, A_{ip} describes the depolarization from just inside the membrane to infinity, ν (which is $\nu = r^2c/[(r + d)^2(c + d)]$ is the volume ratio of the cell exterior to interior, r the cell radius, c the cell half-length, and d is the membrane thickness. In the case of a RBC, d is approximately three orders of magnitude less than r and c, and thus the approximation that $A_{op} = A_{ip}$ can be made, and a useful expansion of this factor can be expressed in terms of $\gamma = c/r$ as shown in [1].

$$A_{op} = A_{ip} = \frac{\left[1 + \frac{3}{5}(1 - \gamma^{-2}) + \frac{3}{7}(1 - \gamma^{-2})^2 + \cdots\right]}{3\gamma^{-2}} \tag{4}$$

For a sphere, $\gamma = 1$, and thus $A_{op} = A_{ip} = 1/3$, which forces this model to converge to the well known spherical CM factor. However, γ does not equal unity for a bRBC, and unless otherwise stated, we use the following well-accepted parameters for a bRBC: $d = 8$ nm, $c = 1.5$ μm, and $r = 3.1$ μm. The membrane conductivity, media conductivity, and cytoplasm permittivity are assumed to be $<10^{-7}$ S/m, 110 μS/cm, and 60, respectively. It is important to note that the value used for the media conductivity here, 110 μS/cm, is significantly different from that presented earlier for 0.85% saline, ~12 mS/cm. This reflects the use of a low-conductivity zwitterion buffer as the suspending medium, and is further described below. Additionally, the membrane permittivity and cytoplasm conductivity are important parameters that will be adjusted and determined experimentally.

2.3 Optimization of buffer solution

Using reported electrical properties for a RBC [15] suspended in a standard 0.85% NaCl solution, cof_1 and cof_2 have been calculated and indicated in Figs. 3A and B. The computed 70 MHz is out of range of most portable function generators, whose maximum frequency typically does not exceed 20 MHz. Perhaps more significant though is that a sensitive frequency scan from cof_1 (1.3 MHz) to cof_2 (70 MHz) would be required in order to determine both cof's, and this would be expected to be a time-intensive process.

We previously introduced the idea of replacing 0.85% saline (and other commonly employed salt solutions or biological buffers) with a low-conductivity and high-permittivity zwitterion buffer as a means of optimizing the buffer solution [16]. Aqueous dielectric modification through zwitterion modification has been well studied [17] and it has been shown that cells exhibit long lasting stability with no signs of cell lysis in such low-conductivity zwitterion solutions [4]. The advantage of utilizing this buffer can be seen through a sensitivity study of the single-shell model in Fig. 2, and summarizes the influence of each parameter on the real part of the CM factor. Based on this study, cof_2 reduction can be accomplished by a simple decrease in the electrolyte relaxation time, $\sigma_{cyto}/\varepsilon_m$, by decreasing cytoplasm conductivity. This can be accomplished through the careful use of a low-conductivity buffer that facilitates osmotic-induced water transport into the cell, or by increasing media permittivity with zwitterions. Figures 3A and B illustrate how the single-shell model predicts both cof's at two different cytoplasm

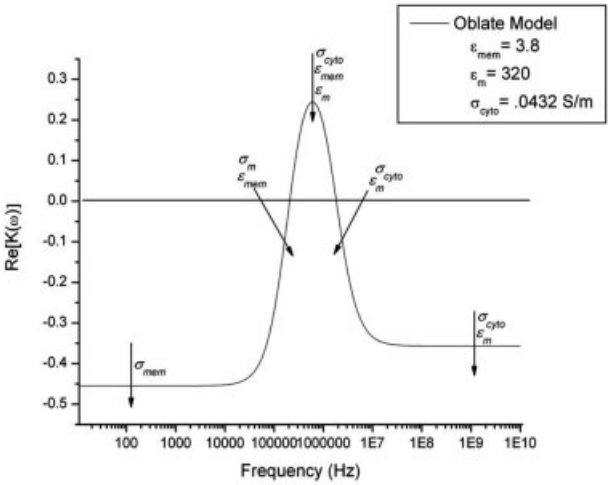

Figure 2. Sensitivity study of the single-shell model parameters on the real part of the Clausius–Mossotti factor $K = Re(f_{CM})$ for the given set of parameters. Change in the electrical parameters gives rise to changes in the CM factor and the cof's as indicated by arrows. The parameters σ_{mem}, ε_m, and ε_{cyto} are taken to be 10^{-7} S/m, 320, and 60.

conductivities for a range of electrolyte permittivities. Based on the single-shell model, the cytoplasm conductivity would have to be decreased by a factor of 10 and electrolyte permittivity increased by a factor of 3 in order to reduce the cof_2 to a more accessible value of approximately 1 MHz. To achieve such a large adjustment, we suspend bRBCs in a low-conductivity high-permittivity zwitterion solution (3 M aminohexanoic acid). This results in an increase in the electrolyte dielectric constant from the standard value of 78.2–320, and the cytoplasm conductivity is decreased from 300 to 30 mS/m due to the cell reaching new osmotic equilibrium with the low-conductivity zwitterion buffer. As shown in Fig. 3, cof_1 remains approximately constant over a large range of media permittivity values around the buffer value and some typical cytoplasm conductivities in our experiment, while cof_2 is greatly reduced from 70 MHz to approximately 1 MHz. To underscore the effect of the new buffer, the cof's for untreated RBCs in PBS (σ_{cyto} = 31 S/m, σ_m = 12.0 mS/cm) and untreated RBCs in our optimized zwitterion buffer (σ_{cyto} = 03 S/m, σ_m = 110 μS/cm) are indicated in Fig. 3.

2.4 RBC membrane cross-linking

Dielectrophoretic probing can be further sensitized through cell surface and/or interior modification. In conjunction with buffer optimization, we previously introduced the use of Glt. cross-linking (cell fixation) in order to amplify membrane and cytoplasm protein content differences in bRBCs allowed to age in 0.85% saline [18]. Glt. treatment cross-links both membrane and interior proteins [19], resulting in a highly stable particle composed of a matrix of polyelectrolytes. bRBC fixation was carried out as it was assumed that as the cell ages within 0.85% saline (which is a nutrient deprived medium, thus causing cell starvation), the protein content on both the cell surface and interior would decrease, consequently leading to a decrease in cytoplasm and membrane cross-linking and correspondingly resulting in a lower cytoplasm conductivity and membrane permittivity. Both of these parameters are expected to impact the measured bRBC cof's as indicated within Fig. 2, and were investigated in greater detail using the previously described single-shell model.

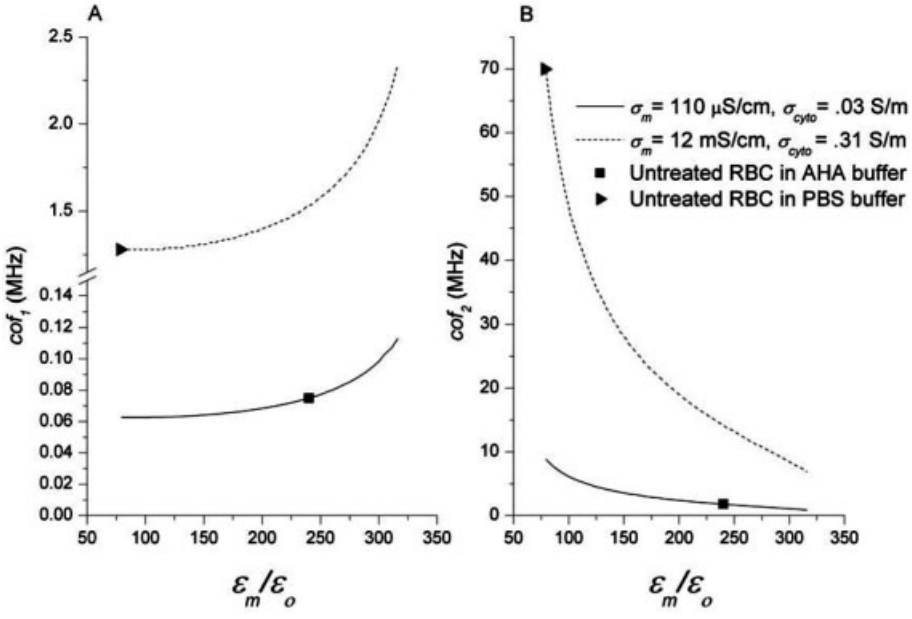

Figure 3. Sensitivity study of the two cof's with respect to the medium dielectric constant. (A) Low-frequency crossover cof_1. (B) High-frequency crossover cof_2. The marked points correspond to untreated RBCs for our buffer and for a standard PBS solution. The parameters σ_{mem}, ε_{mem}, and ε_{cyto} are taken to be 10^{-7} S/m, 10.5, and 60.

3 Materials and methods

3.1 Experimental setup

A quadrupole electrode arrangement was utilized to generate an inhomogeneous electric field that allowed for the observation of the DEP behavior of the RBC samples of interest. These electrodes were fabricated by patterning dual titanium–gold layers onto precleaned 50×75 mm^2 glass slides. These slides were patterned with the image reversal photoresist Shipley AZ-5214 to define the electrode patterns, after which 50 Å of titanium and 2500 Å of gold were evaporated onto the slides. This was followed by a resist dissolution and metal liftoff in acetone. The arrays were designed as four triangular posts with an inner square side length of 25 μm and an electrode width of 60 μm.

The fabricated array, as shown in Fig. 4A, was attached to a function generator set to 10 V_{pp} (Agilent, model #33220A) *via* copper tape and wire leads which yielded the center region of the four electrodes an absolute field minimum and the wire edges an absolute field maximum. A plastic coverslip was then placed over the array followed by RBC sample injection. The entire device was then viewed on a portable epi-flourescent microscope (Labsmith SVM340) and the frequency was slowly increased from 50 kHz to 5 MHz in order to determine both cof values. As shown in Fig. 4B, cof_1 was taken when the RBCs migrated from the electrode center to the electrode edges, while cof_2 was taken when the RBCs migrated back to the array center (Fig. 4C).

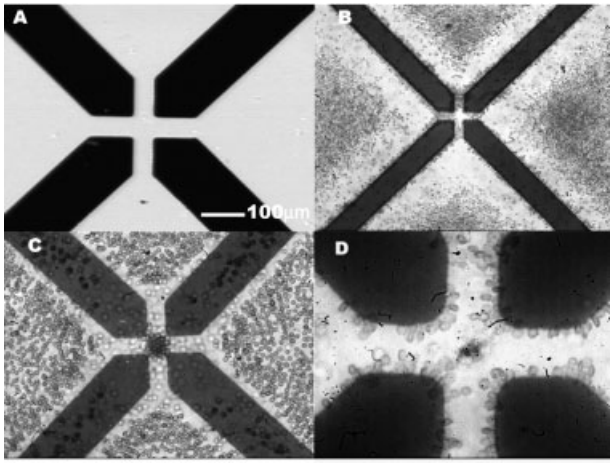

Figure 4. (A) Quadrupole electrode array used in this study. (B) Observed pDEP behavior of RBCs. (C) Observed nDEP behavior of RBCs. (D) Separation of 4 wk old cells (array center) from 1 wk old (edges of wire), image taken at a Glt. concentration of 2.5%, ω = 1.5 MHz.

3.2 Sample preparation

bRBCs (Quad Five, Cat. #943) were allowed to age at 4°C within a 0.85% saline suspension (thus under starvation conditions) and aliquots were removed at specific time points (0, 1, 2, and 4 wks) for Glt. cross-linking and finally DEP analysis. This particular experimental work (with bRBCs) was described in a previous publication [12] and thus will not be discussed in detail here. Briefly, after removing the aliquot from the bRBC stock suspension, the cells were washed and resuspended in 3 M AHA. The suspension was then split into several 2 mL aliquots within individual 15 mL centrifuge tubes. The cross-linking reaction was then initiated through the addition of an appropriate amount of Glt. (producing solutions with Glt. concentrations of 0, 0.06, 0.1, 0.3, 0.6, 1, and 2.5%) to the suspension, and the reaction was allowed to proceed for 30 min under conditions of gentle mixing. Following this 30 min reaction period, the cell fixation was halted through washing once with 3M sodium borohydride (Sigma Cat#213462), three times with PBS (pH 7.4) and then once with the zwitterion 3 M aminohexanoic acid (AHA, pH 6.9, Sigma, Cat #A7824). The dielectric constant of this zwitterion buffer has been previously reported at 320 [17] and its conductivity was measured to be 110 μS/cm. After this final wash, the cells were resuspended in 3 M AHA and immediately analyzed for their DEP response.

4 Results and discussion

Based on earlier arguments, we expect the cytoplasm conductivity and the membrane permittivity to be responsible for the difference in cof's. To discern how cross-linking and age affect both parameters, the cof's from the oblate shell model are plotted in Fig. 5 for typical values of both parameters. As expected from earlier discussions on the relaxation times and from Fig. 2, cof_1 is sensitively affected by the membrane permittivity while cof_2 by cytoplasm conductivity, while the sensitivity to the other parameter is negligible by comparison for each of the two cof's. The dependence of cof_2 on cytoplasm conductivity is roughly linear, as seen in Fig. 5D, such that a 0.02 S/m difference in the cytoplasm conductivity, roughly a factor of two change in its value, can produce a 1 MHz difference in cof_2. Exploiting this fact, a mixed suspension of 50% 4 wk old and 50% 1 wk old cells, fixed at a Glt. concentration of 2.5%, was placed on the quadrapole array, and the resulting old and young cells were separated at a frequency of 1.5 MHz, as shown in Fig. 4D.

cof measurements for RBC age times of 1, 2, and 4 wks are shown in Figs. 6 and 7. Both high- and low-frequency cof's at different Glt. concentrations are measured for bRBCs at 1, 2, and 4 wks of age. Untreated RBCs had measured cof_1 and cof_2 values of 75 kHz and 1.8 MHz, respectively with no variance with RBC age. Therefore, without cell fixation treatment, no discernable difference in RBCs of differing starvation age can be distinguished using DEP, which has about a 50 kHz resolution.

Upon RBC fixation at a low-Glt. concentration of 0.06%, an increase in cof_1 from 75 kHz to 220, 220, and 225 kHz was observed for RBC starvation age groups of 1, 2, and

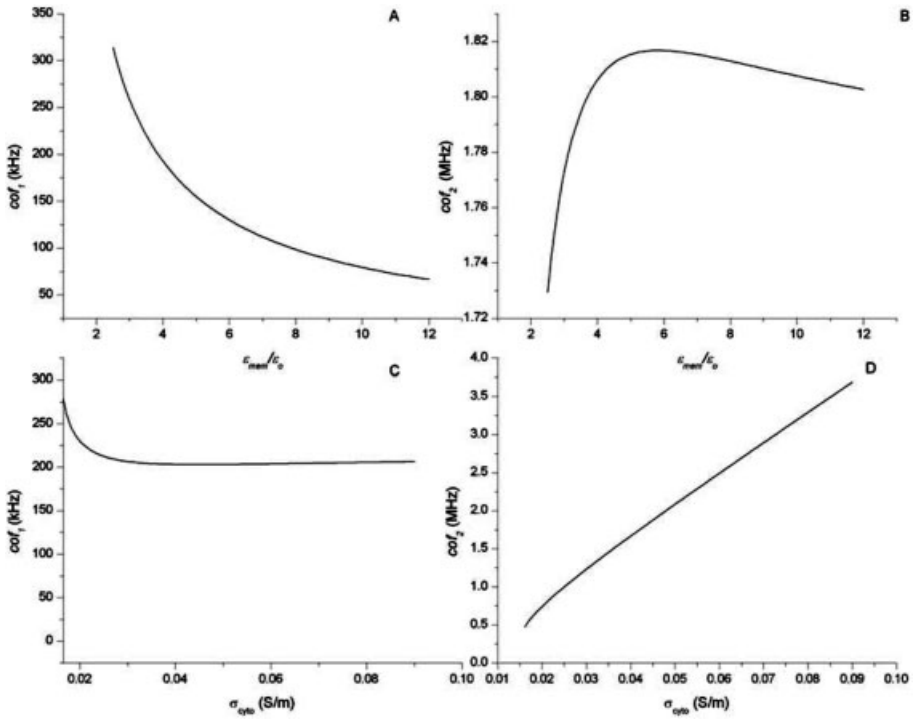

Figure 5. (A, B) Sensitivity of cof_1 (A) and cof_2 (B) with respect to membrane dielectric constant at σ_{cyto} = 0.03 S/m. (C, D) Sensitivity of both cof's to cytoplasm conductivity at ε_{mem} = 3.8 for (C) cof_1 and (D) cof_2.

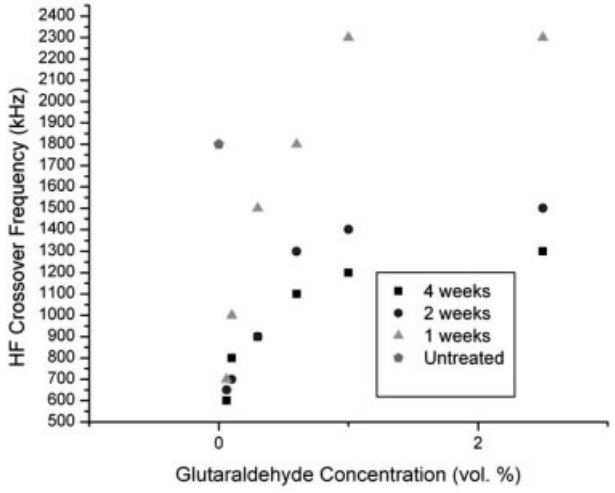

Figure 6. Experimentally measured cof_2 as a function of the cell starvation age and Glt concentration.

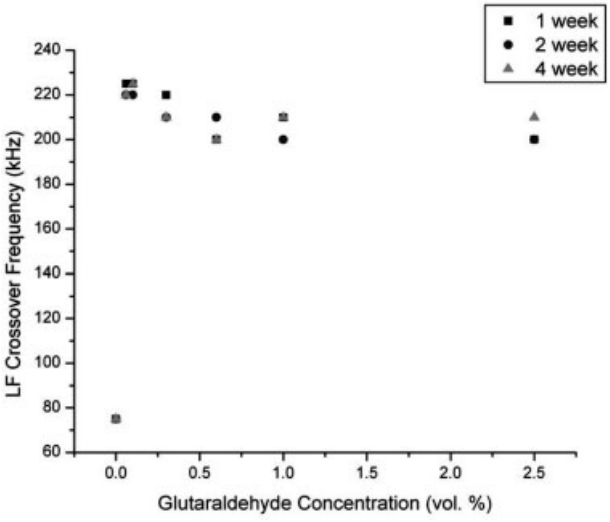

Figure 7. Experimentally measured cof_1 as a function of the cell starvation age and Glt. concentration.

4 wks, respectively, with all three groups reaching a maximum value of 225, 220, and 225 kHz, respectively at a Glt. concentration of 0.06%. There is hence little age-sensitivity, but a large dependence on the Glt. concentration at low concentrations. Similarly, a decrease in cof_2 from 1.8 MHz to 600 kHz was observed in all three age groups at low-Glt. concentrations. After this sharp decrease following the introduction of a slight amount of Glt., cof_2 of the 4- and 2-wk old RBCs had a small difference of about 50 kHz. There is hence enhanced, but still weak, starvation age sensitivity in cof_2 at low concentrations. However, as Glt. concentration was steadily increased from 0.06 to 2%, cof_1 was observed to slowly decrease to a constant value of ~210 kHz for all three RBC age groups, while cof_2 was observed to steadily increase and reached an age-dependent asymptote of 2.3, 1.5, and 1.3 MHz for RBC ages of 1, 2, and 4 wks, respectively. The first value is higher than the untreated RBC, suggesting that the cytoplasm of highly treated young RBCs can be higher than that of untreated RBCs. Increasing Glt. concentration

beyond 2% did not change the respective cof_2 significantly. The high-concentration asymptotes of cof_2 are hence most sensitive to the RBC age, with at least a factor of 2 increase in the difference in the cof_2 for RBCs of different age. (The untreated 1, 2, and 4 wk old RBCs do not have discernable difference in cof_2 within the 50 kHz measurement resolution whereas the difference of their asymptotic values at high-Glt. concentration is 1 MHz)

Based on Fig. 5 and earlier arguments, small amounts of Glt. (below 0.1%) must hence reduce the membrane permittivity, but this value remains constant beyond 0.1% Glt. We estimate the relative membrane permittivity is reduced from 10.5 to 3.8 by evaluating the jumps in the cof_1 for all three RBCs with different age. This reduction in membrane permittivity is not sufficient to account for the decrease in cof_2 at 0.1% Glt. There must hence be a decrease in cytoplasm conductivity at low concentrations.

At Glt. concentrations beyond 0.1%, Figs. 5 and 6 indicate that Glt. increases the cytoplasm conductivity steadily until it also reaches an asymptotic value beyond 2%. We estimate the largest range in cytoplasm conductivity beyond 2% Glt. to be from 0.068 to 0.1 S/m. This represents a 1 MHz difference in cof_2, as seen in Fig. 5D, as is consistent with our measured cof_2 difference in Fig. 6. Conversely, the same cof_2 data would suggest that the difference in cytoplasm conductivity of untreated RBCs to be no more than 2 mS/m, or less than 1% of its value. To verify this observation, we estimate the cytoplasm conductivity of cells of different age at different Glt. concentrations from cof_2, and use this value to estimate cof_1 at the same conditions with a relative membrane permittivity of 3.8. As seen in Fig. 8, this predicted cof_1 is in agreement with all of our measured cof_1 data at different age and different Glt. concentrations beyond 0.1%. Treated blood cells of different age definitely possess different cytoplasm conductivities.

Since the sensitivity of cof_1 at below 0.1% Glt. concentration does not amplify the sensitivity in cell starvation age, we deduce that the cell age does not affect the membrane permittivity with or without the cross-linking reaction. That high-Glt. concentration can amplify the difference in cof_2 for cells of different age, on the other hand, indicates that age can profoundly affect the cytoplasm conductivity of treated cells, but only marginally for untreated ones. The slightly higher cytoplasm conductivity (no more than 1%) of younger untreated cells, if it is there, is expected to be because of more active ion-channel and ion-pump activity that maintains a higher ionic strength within the cell. However, a totally different mechanism must be responsible for the significantly higher cytoplasm conductivity of younger-treated cells.

It is well known that Glt. treatment removes the majority of positive amino groups from the RBC membrane surface during cross-linking [20]. It is reasonable to expect such cleaving of amino groups to also occur on the interior membrane interface, thus releasing ions into the cytoplasm and increase its conductivity. It is expected that the initial de

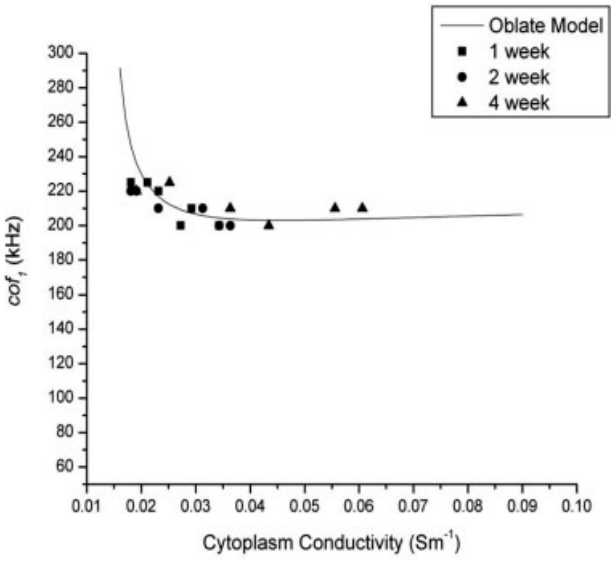

Figure 8. Collapse of cof_1 data for different cell age and at different Glt concentrations by estimating the cytoplasm conductivity from cof_2.

crease in cytoplasm conductivity at low-Glt. concentrations is due to ion flux out of the cell, as Glt. is known to freeze these channels open, inhibiting the cell to regulate ion flux. However, higher Glt. concentrations are likely to prevent such flux as the degree of cross-linking reaches a point where the crosslinked membrane protein matrix blocks the ion channels. The observed concurrent sensitivity of the cytoplasm conductivity to both cell age and cross-linking is also reasonable if one takes into account that, as RBCs age in nutrient-lacking media, the breakdown and vessication of reactant limiting membrane amino groups takes place [21]. Younger, healthier cells exposed to shorter starvation times are expected to have a larger, but finite amount of available surface groups that can be cleaved during cross-linking. Without cross-linking, however, the excess amino groups are not mobile and hence cannot change the cytoplasm conductivity. The asymptotic cof_2 in Fig. 6 may hence represent the total number of available surface groups for Glt. cleavage during cross-linking – a titration limit. This is consistent with the fact that, as shown in Fig. 3, younger 1 wk old-treated cells have a higher cytoplasm conductivity than untreated RBCs. As the RBC increases in starvation age, the available surface groups within the cell interior decrease, thus giving rise to a reduced number of surface reactants available to be cleaved during cross-linking, and a decrease in cytoplasm conductivity occurs at the same Glt. concentrations. Hence, the larger difference (ten times) in the cytoplasm conductivity of young and old cells is due to the much larger numbers of cleavable amino groups in younger cells. It is hence unrelated to ion channel activity and its effect on cof_2 cannot be realized unless cross-linking reaction by Glt. releases amino groups into the interior of the cell.

5 Concluding remarks

An optimized dielectrophoretic buffer with cross-linking agent has been developed for the detection of RBC age. A dielectric model had been tailored to fit the experimental data of bRBCs of varying starvation age. The experimental results demonstrate that it is possible to identify and separate RBCs of varying starvation age. In the absence of zwitterion buffer and Glt. cell fixation, no discernable differences in cof measurements exist. Additionally, cof_2 is predated to be approximately 70 MHz, well above the capabilities of conventional AC function generators. An order of magnitude decrease in this value was achieved through the reduction in cytoplasm conductivity and media dielectric constant by resuspending the RBCs into a low-conductive nonlysing electrolyte buffer. Additionally, differences in membrane properties, initially indistinguishable amongst RBCs of differing age were made apparent through a Glt. fixation reaction, which changes the cytoplasm conductivity by cleaving more amino groups from younger cells. Such optimization schemes suggest the possibility that novel DEP detection assays can be tailored to specific subgroups of a biological systems, such as malarial infected RBCs or sickle cell anemia, both cases where the membrane properties (number of surface amino groups) of the infected cell differ substantially from their healthy counterpart.

The authors have declared no conflict of interest.

6 References

[1] Pohl, H. A., *Dielectrophoresis the Behavior of Neutral Matter in Nonuniform Electric Fields*, Cambridge University Press, Cambridge 1978.

[2] Green, N. G., Ramos, A., Morgan, H., *J. Phys. D Appl. Phys.* 2000, *33*, 632–641.

[3] Green, N. G., Morgan, H., *J. Phys. D Appl. Phys.* 1997, *30*, L41–L44.

[4] Arnold, W. M., *IEEE Trans. Ind. Appl.* 2001, *37*, 1468–1475.

[5] Cheng, I. F., Chang, H. C., Hou, D., Chang, H. C., *Biomicrofluidics* 2007, *1*, 021503-021501–021503-021515.

[6] Wang, X. B., Huang, Y., Gascoyne, P. R. C., Becker, F. F. *et al.*, *Biochim. Biophys. Acta* 1994, *1193*, 330–344.

[7] Wang, X. J., Becker, F. F., Gascoyne, P. R. C., *Biochim. Biophys. Acta* 2002, *1564*, 412–420.

[8] Gascoyne, P. R. C., Pethig, R., Burt, J. P. H., Becker, F. F., *Biochim. Biophys. Acta* 1993, *1149*, 119–126.

[9] Markx, G. H., Dyda, P. A., Pethig, R., *J. Biotechnol.* 1996, *51*, 175–180.

[10] Pethig, R., Talary, M. S., *IET Nanobiotechnol.* 2007, *1*, 2–9.

[11] Markx, G. H., Zhou, X. F., Pethig, R., *Electrostatics 1995* 1995, 145–148.

[12] Gordon, J. E., Gagnon, Z., Chang, H.-C., *Biomicrofluidics* 2007, *1*, 044102-044101–044102-044105.

[13] Hoeber, T. W., Hochmuth, R. M., *Mech. Eng.* 1970, *92*, 604.

[14] Irimajiri, A., Hanai, T., Inouye, A., *J. Theor. Biol.* 1979, *78*, 251–269.

[15] Gascoyne, P., Satayavivad, J., Ruchirawat, M., *Acta Trop.* 2004, *89*, 357–369.

[16] Gagnon, Z., Chang, H. C., *Electrophoresis* 2005, *26*, 3725–3737.

[17] Arnold, W. M., Zimmermann, U., *Biochem. Soc. Trans.* 1993, *21*, 475S.

[18] Gordon, J. G., Gagnon, Z., Chang, H. C., *Biomicrofluidics* 2007, *1*, 044102.

[19] Heard, D. H., Seaman, G. V. F., *Biochim. Biophys. Acta* 1961, *53*, 366–374.

[20] Georgieva, R., Neu, B., Shilov, V. M., Knippel, E. *et al.*, *Biophys. J.* 1998, *74*, 2114–2120.

[21] Greenwalt, T. J., Dumaswala, U. J., *Br. J. Haematol.* 1988, *68*, 465–467.

